

New Perspectives for Infrared Imaging Enabled by Colloidal Quantum Dots

Paweł E. Malinowski¹, Vladimir Pejović¹, Abu Bakar Siddik¹, Itai Lieberman¹, Joo Hyung Kim¹, Tristan Weydts¹, Myung Jin Lim¹, Luis Moreno Hagelsieb¹, Naresh Chandrasekaran¹, Antonia Malainou¹, Gauri Karve¹, Isabel Pintor Monroy¹, Wenya Song¹, Sangyeon Lee¹, Nikolas Papadopoulos¹, Jonas Bentell¹, Zohreh Zahiri¹, Steven Thijs¹, Arman Uz Zaman¹, Marina Vildanova¹, Jiwon Lee^{1,2}, David Cheyns¹, Paul Heremans¹

¹ Imec

Kapeldreef 75, Leuven, Belgium

² POSTECH, Pohang University of Science and Technology

77 Cheongam-ro, Nam-gu, Pohang-si, Gyeongsangbuk-do, South Korea

E-mail: Pawel.Malinowski@imec.be

Abstract Colloidal quantum dots can be monolithically integrated with the readout circuit, enabling high resolution and high pixel density. With tunable bandgap, they can extend the functionality of CMOS image sensors beyond Si cut-off wavelength, into the short- and mid-wave infrared regions. In this talk, we will review next generation technology opportunities such as Pb-free absorbers, multispectral architectures and low-noise pixel design. We will also take a look at promising use cases in industrial machine vision, automotive and space applications.

Keywords: infrared, SWIR, image sensor, photodetector, QD, quantum dot

1. Introduction

Image sensors have become an essential part of most categories of electronic devices. Next to imaging, which targets as good as possible replication of human vision, sensing is gaining traction. Here, acquisition of specific information trumps esthetics of photography. One of the trending topics in sensing is infrared sensing, especially in the short-wave infrared (SWIR, Fig. 1), which can provide new information beyond human vision. Up to now, this modality has been limited to high-end applications, justified by very high cost of the sensor based on III-V and II-VI materials manufactured with high-temperature epitaxial growth at low throughput, and then hybridized to the readout chip typically by die-to-die bonding. With the advent of disruptive technologies that can support wafer-level, semiconductor-fab-compatible manufacturing, the SWIR range can finally be democratized with sensors manufactured at cost approaching CMOS image sensors once high volume capacity becomes more established. In this paper, we focus on colloidal quantum dot (CQD) image sensors that are enabling new types of infrared image sensors while maintaining fab compatibility [2,3].

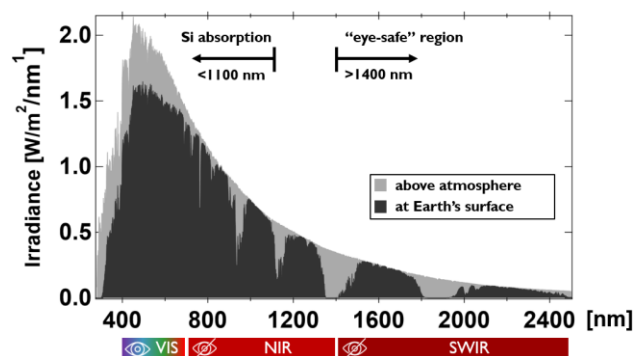


Fig. 1. Solar irradiance above atmosphere (grey) and at Earth's surface (black), showing characteristic peaks and valleys associated with water absorption windows.

Among the target applications, automotive use cases are under consideration (Fig. 2). In-cabin driver monitoring systems (DMS) could take advantage of SWIR sensing by enabling visibility through sunglasses (to maintain monitoring of eyes for driver drowsiness detection), visibility through smoke (to see the state of driver and passengers even in case of vaping) and robustness to solar glare (by operating at a solar minimum or in a solar blind mode). Out-of-cabin advanced driver-assistance systems (ADAS) and autonomous driving (AD) systems could benefit from improved visibility through fog/smoke/mist, higher contrast of animals and pedestrians and detection of ice/water on the road, especially in corner cases. Other sectors include consumer electronics (e.g. eye-safe eye trackers for AR/VR headsets), industrial machine vision (e.g. sorting), remote sensing (e.g. crop monitoring), security (e.g. miniaturized surveillance cameras) and defense (e.g. compact cameras for unmanned drones). According to Yole [1], SWIR camera market will grow at 44% CAGR to reach 2.9B\$ market size by 2028 (from 322M\$ market in 2022). CQD technology is identified as one of the gamechangers, with interesting dynamics already happening (onsemi acquiring SWIR Vision Systems, Lynred acquiring NIT, Sony introducing both InGaAs and InAs QD advancements [4,5]).



Fig. 2. Example applications in the automotive domain: driver monitoring system (left) and ADAS/AD system (right).
Generated using MS Copilot for illustration purposes only.

2. Thin-film photodetector platform

Image sensors using thin-film photoactive layers should be seen as a new technology platform that can be customized depending on the application. A stack of materials (each with submicron thickness) are built monolithically on top of the readout circuit (which can be based on CMOS or TFT, Fig. 3). Each stack contains at least the absorber layer (which can be colloidal quantum dots, organic – polymers or small molecules, or perovskite). This layer is sandwiched between electron and hole transport layers (ETL/HTL), and their order defines the polarity of the photodiode. Additional layers such as light manipulating ones (e.g. metasurfaces below or filters above) or encapsulation can be further added to adjust specific features. The photodiode and pixel can be tuned largely separately, and the spatial metrics (e.g. pixel size or resolution) are defined only by the underlying readout technology.

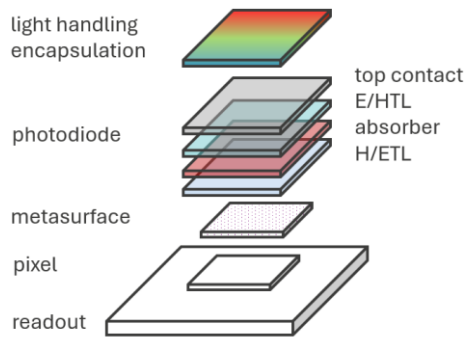


Fig. 3. Schematic of the thin-film photodetector (TFPD) platform: multi-layer stack including photoactive absorber layer (e.g. QD, OPD, PePD) monolithically integrated on readout.

3. Quantum dot photodiode stack

Majority of CQD sensor implementations up to now has been using PbS as the absorber material. With that, several milestones have been demonstrated, validating maturity, manufacturability and customizability of this new image sensor technology. External quantum efficiency above 80% at 1400 [6], pixel size below 2 μm for hi-res sensors fabricated on 300 mm wafers [7], 6 MPx sensors [8] or eSWIR functionality up to 2 μm wavelength [9] are some of breakthrough achievements.

Fig. 4 shows an example of the EQE spectrum for two PbS QDPD devices. With adjustments of the stack (bottom reflector, transport layers type and thickness, absorber thickness, transparent top contact, etc.), it was possible to boost the EQE at ~ 1400 nm to 70% from the reference value of $\sim 40\%$. One can note differences in the rest of the spectrum.

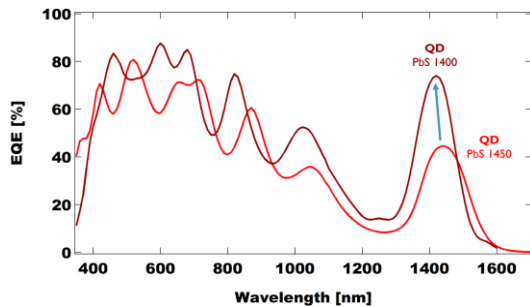


Fig. 4. External quantum efficiency vs. wavelength for a PbS QDPD fabricated on Si substrate (illumination through a transparent top contact). Light red curve shows initial result and dark red curve the result after optimization for high sensitivity at the peak at the 1400 nm wavelength band.

While PbS has been instrumental as a breakthrough material to enable first products and showcase unique platform possibilities, we consider it a 1st generation QD absorber (Fig. 5). The next step for wider deployment (fab compatibility, RoHS acceptance and environmental policy fit) is switching to Pb-free absorbers (2nd generation).

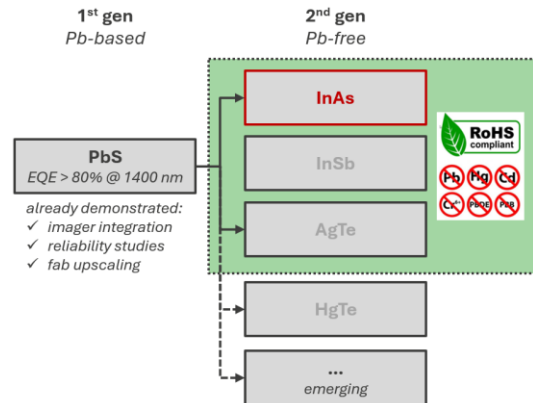


Fig. 5. Two generations of QDPD absorbers: PbS (1st gen) and Pb-free (2nd gen) with examples of materials under development.

Most notable contender seems to be InAs, promising also higher response speed (sub-ns) and better reliability. There continues to be a rapid progress on improving the EQE, with 79% at 940 reported [10]. Our results already cross the barrier of 30% EQE at 1250 nm (Fig. 6) for top-illuminated stacks on Si substrate, compatible with ROIC integration [11]. Dark current density is still under improvement, with 30 $\mu\text{A}/\text{cm}^2$ at -3V bias for these initial devices. Other candidates being investigated are InSb (especially for cut-off wavelength extension [12]), AgTe (with recent imager proof-of-concept demonstration [13]) and HgTe (interesting for the MWIR range, but not RoHS compatible [14]).

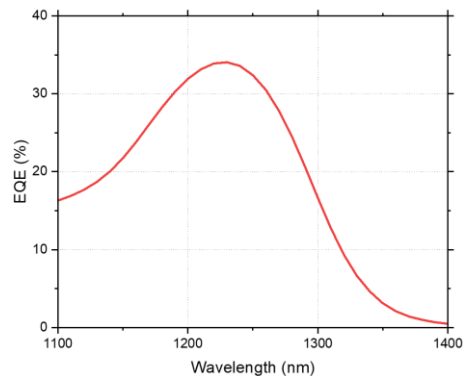


Fig. 6. External quantum efficiency vs. wavelength at -3 V reverse bias voltage for an InAs QDPD fabricated on Si substrate (illumination through a transparent top contact).

4. Pixel and readout circuit

On the readout side, initial research started with TFT pixels [15], but the focus quickly shifted to CMOS architecture. This was to leverage wafer-level manufacturing possibilities with increasing maturity of the technology and improving compatibility with more standard semiconductor fab process flows. Many implementations take advantage of ROICs typical for InGaAs detectors [16] such as capacitive trans-impedance amplifier (CTIA) providing good control of low bias voltage, enabling lower dark current from the detector.

Pixel architecture facilitating compact footprint is the common “3T” type (Fig. 7), with the QDPD stack integrated directly on top of the metal contact connected to the source-follower circuit in the chip. This baseline concept is the simplest to realize, but the resulting sensor suffers from high dark current and detrimental kTC noise.

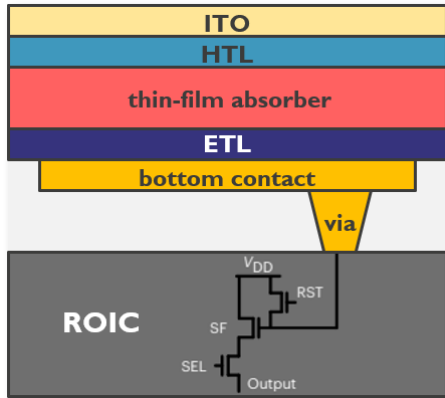


Fig. 7. Schematic cross-section of a “3T” (3-transistor) pixel stack, with one metal contact per pixel.

One of the benefits of 3T pixels is the possibility of achieving a high pixel density, with demonstrations of pixel size approaching the target detection wavelength (1.82 μm [17], 1.62 μm [7], Fig. 8). A FullHD (1920x1080 px) focal plane array with the latter pixel size would be only $\sim 5.5 \text{ mm}^2$, yielding even around 1000 image sensors from one 12 inch wafer.

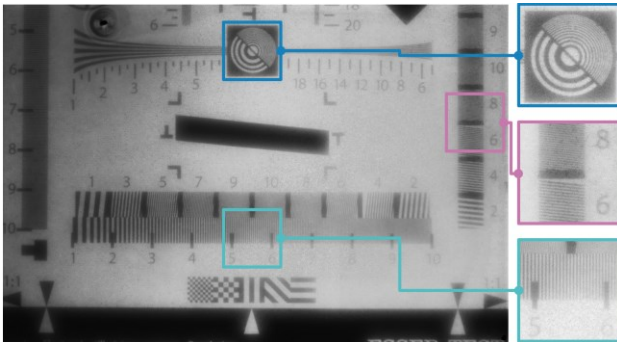


Fig. 8. Example of an image acquired with a PbS-based image sensor optimized for high pixel density: 1536x1024 pixels, 1.62 μm pixel pitch.

We presented an alternative “4T” pixel approach (Fig. 9 [18]) by adding a TFT (using IGZO as the channel material) in the back-end-of-line (BEOL). This has been inspired by the breakthroughs in CCD and CMOS image sensors realized by invention of the pinned photodiode (PPD) structure [19,20], and starting the revolution in imaging. The PPD architecture allows for kTC noise cancellation with correlated double sampling by transferring all charges from the photodiode to the floating diffusion node.

In our first implementation of the thin-film PPD (TF-PPD), we observed reduced kTC noise, increased conversion gain (CG), lower dark current and increased photodiode full-well capacity. The advantages of the resulting higher image quality were verified with test arrays of 64x64 pixels (5 μm pitch) by comparing 3T and 4T devices with the same photodiode stack and measurement conditions (Fig. 10).

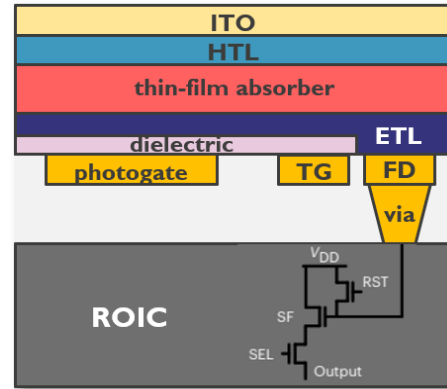


Fig. 9. Schematic cross-section of a “4T” (4-transistor) pixel stack, with an additional thin-film transistor (TFT) fabricated in the back-end-of-line (BEOL) of the CMOS readout.

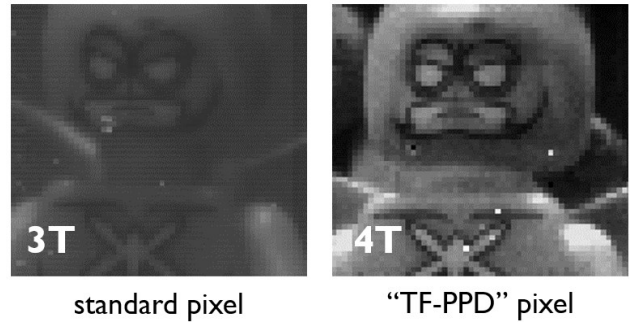


Fig. 10. Images acquired with the same settings and with the same (NIR OPD) photodiode stack on 3T (left) and 4T pixel (right), showing higher sensitivity of the latter architecture.

5. Multi-band selectivity

The initial demonstrations of QD-based image sensors have one stack covering the entire focal plane array (FPA), which means that all pixels have the same spectral response. This also means that the resulting imager has a broadband response, as QDs show sensitivity throughout the “bulk” visible range, extended all the way to the cut-off wavelength defined by the nanocrystal size [21]. There are several approaches to realize wavelength band distinction per region or per pixel, including: stacking QDs of different size, side-by-side QD stacks, or filters on top of the stack. We have been developing a new approach based on metasurfaces fabricated as a part of the standard fab BEOL process (Fig. 11 [22]). In this way, each pixel of the array can have a dedicated wavelength response by tuning the effective refractive index with a scalable design of the flat optics element under the QD pixel stack. In this “multispectral by design” concept, the peak response can be adjusted by adjusting one process module according to the requirements of the application, and with keeping a single QD stack everywhere.

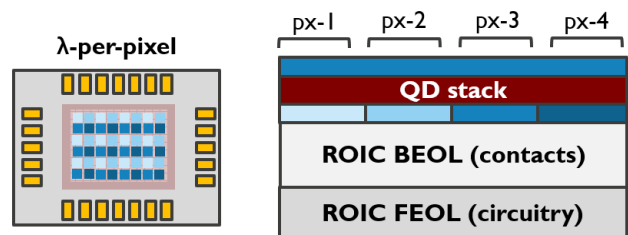


Fig. 11. Schematic (left: top view; right: cross-section) of a per-pixel microcavity approach for realization of multi-band focal plane arrays with a single photodiode stack.

Initial results from single-pixel test structures (Fig. 12) are encouraging, and the proof-of-concept devices are realized with wavelength tunability demonstrated with a PbS stack. This paves the way towards compact, multi-band / multispectral SWIR image sensors with improved performance for object/material/tissue detection.

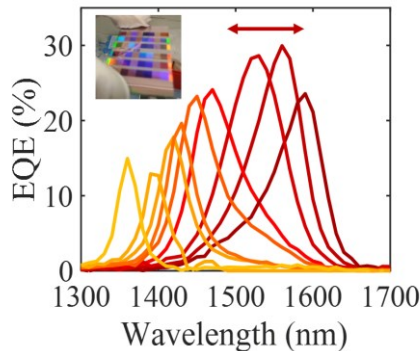


Fig. 12. Initial results of the microcavity approach applied to a single PbS QD stack, showing tunability of the main EQE peak by design of the bottom flat optics module.

6. Reliability

As performance is nothing without sufficient reliability in the final use case scenarios, robustness assessment and improvement has been gaining importance as soon as QD image sensor maturity reached inflection point. Quantum dots are known to be more “fragile” than the traditional semiconductors, and especially sensitivity to high temperatures and humidity raises concerns both for the manufacturing and for the products. Table 1 lists some critical reliability tests that need to be performed for the QD stack and integrated image sensor to verify their suitability for the final application. Automotive applications present the most stringent requirements and are used as guidelines in our reliability investigations [23,24].

Table 1. Examples of reliability tests

Test	Conditions (100s hours)
High temperature stress (HTS)	125°C dry storage
Thermal cycling (TC)	-40°C ↔ 125°C
Damp heat test (DH)	85°C / 85% relative humidity
High Temperature Operating Life Test (HTOL)	70°C dark/illuminated
Mechanical	Package level (e.g. vibration)
Irradiation	App. specific (e.g. X-ray, proton, α , γ for space)

One example of a relatively unexplored territory are irradiation tests with the target of verifying suitability of QD image sensors in space. With the advent of “new space” applications (e.g. CubeSats), availability of miniaturized and low-cost SWIR sensors gains in importance, and stability under harsh conditions is a critical enabler. In our research, we are investigating different types of radiation that will need to be considered once QD sensors are candidates for flight hardware. Initial testing aims at understanding the fundamental principles of degradation and measures to mitigate these effects. Fig. 13 illustrates encouraging results for X-ray irradiation with total ionizing dose (TID) of 220 krad(Si) of a PbS QD SWIR image sensor. In this test, we have not noticed any meaningful degradation of sensitivity, which is promising for further

implementations in low-Earth orbit.

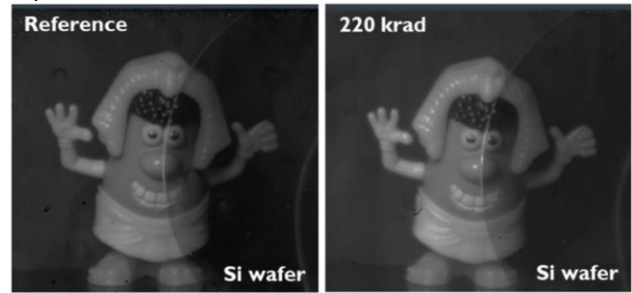


Fig. 13. Image acquired with a PbS image sensor (768x512 pixels, 5 μ m pixel pitch), before (left) and after (right) 220 krad(Si) X-ray irradiation.

7. Conclusions

Colloidal quantum dots should be seen as an enabler for realization of a new image sensor platform. With monolithic, wafer-level integration of thin-film photodiode stacks on readout, cost in mass production can approach single digit values. This could dramatically lower the barrier for implementation of infrared imaging even in consumer applications. Ongoing developments on Pb-free stacks, low-noise 4T pixels and metasurface-based “multispectral by design” arrays show the path towards customizable imagers. Initial reliability assessments are encouraging, but significant effort is needed especially if automotive applications are to be considered. With these and other technological disruptions, the vision of accessible, compact, multifunctional SWIR image sensors with new functionalities is in sight (Fig. 14).

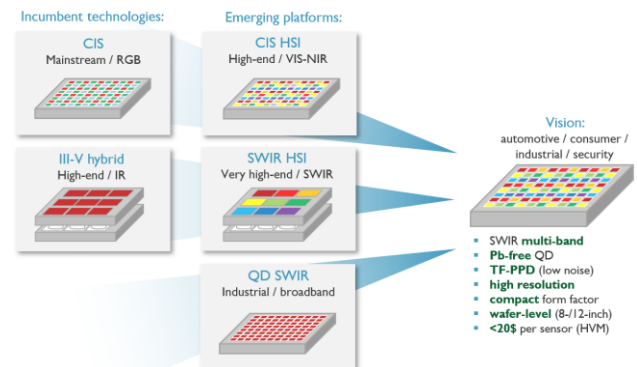


Fig. 14. Vision for the QD imager platform, indicating which modules are critical enablers from the incumbent technologies, and what architecture might open completely new use cases with accessible, miniaturized, multispectral SWIR imaging.

References

- [1] “SWIR Imaging 2023”, Yole Intelligence market report (YINTR23327).
- [2] P.E. Malinowski et al. "Image sensors using thin-film absorbers", *Appl. Opt.* 62(17), F21-F30 (2023) 10.1364/AO.485552
- [3] V. Pejovic et al., “Infrared colloidal quantum dot image sensors,” *IEEE Trans. Electron. Devices* 69, 2840–2850 (2022).
- [4] S. Manda et al., *IEEE International Electron Devices Meeting*, 16-7, DOI: 10.1109/IEDM19573.2019.8993432 (2019).
- [5] O. Enoki et al., “Pb-free Colloidal InAs Quantum Dot Image Sensor for Infrared”, *IEEE International Electron Devices Meeting*, paper 41-7 (2024)
- [6] M. Vafaie et al., “Colloidal quantum dot photodetectors with

- 10-ns response time and 80% quantum efficiency at 1,550 nm,” *Matter*, vol. 4, no. 3, pp. 1042–1053, Mar. 2021, doi: 10.1016/j.matt.2020.12.017.
- [7] J. Steckel et al., “1.62 μm global shutter quantum dot image sensor optimized for near and shortwave infrared,” in *IEDM Tech. Dig.*, Dec. 2021, pp. 23–24, DOI: 10.1109/IEDM19574.2021.9720560
- [8] Acuros 6: <https://www.swirvisionsystems.com/>
- [9] Emberion VS20: <https://www.emberion.com/>
- [10] D. Shin et al., "High Performance Infrared InAs Colloidal Quantum Dot Photodetector with 79% EQE Enabled by an Extended Absorber Layer", *Adv. Optical Mater.* 2401931 (2024), DOI: 10.1002/adom.202401931
- [11] W. Song et al., “Lead-Free Quantum Dot Photodiodes for Next Generation Short Wave Infrared Optical Sensors”, *IEEE International Electron Devices Meeting*, paper 41-8 (2024)
- [12] H. Seo et al., “Colloidal InSb Quantum Dots for 1500 nm SWIR Photodetector with Antioxidation of Surface”, *Adv. Sci.* 2024, 11, 2306439, DOI: 10.1002/advs.202306439
- [13] Y. Wang et al., „Silver telluride colloidal quantum dot infrared photodetectors and image sensors”, *Nat. Photon.* 18, 236–242 (2024), DOI: 10.1038/s41566-023-01345-3
- [14] B. Wang et al. “Short-Wave Infrared Detection and Imaging Employing Size-Customized HgTe Nanocrystals,” *Small Methods* 2301557 (2024), DOI: 10.1002/smt.202301557
- [15] T. Rauch et al., “Near-infrared imaging with quantum-dot-sensitized organic photodiodes,” *Nature Photon.*, vol. 3, no. 6, pp. 332–336, Jun. 2009, doi: 10.1038/nphoton.2009.72.
- [16] C.-C. Hsieh et al., “Focal-plane-arrays and CMOS readout techniques of infrared imaging systems,” *IEEE Trans. Circuits Syst. Video Technol.*, vol. 7, no. 4, pp. 594–605, Aug. 1997, doi: 10.1109/76.611171
- [17] J. Lee et al., “Imaging in short-wave infrared with 1.82 μm pixel pitch quantum dot image sensor,” in *IEDM Tech. Dig.*, Dec. 2020, pp. 343–346, doi: 10.1109/IEDM13553.2020.9372018.
- [18] J. Lee et al., “Thin-film image sensors with a pinned photodiode structure”, *Nat. Electron.* 6, pages 590–598 (2023), DOI: 10.1038/s41928-023-01016-9
- [19] N. Teranishi et al. "No image lag photodiode structure in the interline CCD image sensor". 1982 International Electron Devices Meeting 324–327 (1982).
- [20] E. Fossum et al., "CMOS image sensors: electronic camera-on-a-chip", *IEEE Trans. Electron Devices* 44, 1689–1698 (1997).
- [21] Z. Hens, & J. De Roo “Atomically precise nanocrystals”, *Journal of the American Chemical Society*, 142(37), 15627-15637 (2020), DOI: 10.1021/jacs.0c05082
- [22] V. Pejovic et al., “Spectral and polarization sensing in short-wave infrared with thin-film photodiodes and optical metasurfaces” *Proceedings Volume 13083, SPIE Future Sensing Technologies 2024*; 1308310 (2024) DOI: 10.1117/12.3022596
- [23] AEC-Q100: www.aecouncil.com
- [24] JEDEC Standard No. 22-A101: www.jedec.org
- [25] M. Jin et al., “Effect of X-Ray Irradiation on Colloidal Quantum Dot SWIR CMOS Image Sensor”, *IEEE Transactions on Electron Devices*, Volume: 71, Issue: 1 (2024), DOI: 10.1109/TED.2023.3329452